Journal of Magnetic Resonance 276 (2017) 122–127

Contents lists available at ScienceDirect

Journal of Magnetic Resonance

journal homepage: www.elsevier.com/locate/jmr

Communication

High field hyperpolarization-EXSY experiment for fast determination of dissociation rates in SABRE complexes

Niels K.J. Hermkens, Martin C. Feiters, Floris P.J.T. Rutjes, Sybren S. Wijmenga, Marco Tessari *

Radboud University, Institute for Molecules and Materials, Heyendaalseweg 135, 6525 AJ Nijmegen, The Netherlands

ARTICLE INFO

Article history:
Received 2 December 2016
Revised 16 January 2017
Accepted 17 January 2017
Available online 21 January 2017

Keywords:
Hyperpolarization
SABRE
Exchange
Dissociation rate

ABSTRACT

SABRE (Signal Amplification By Reversible Exchange) is a nuclear spin hyperpolarization technique based on the reversible concurrent binding of small molecules and *para*-hydrogen (p-H_2) to an iridium metal complex in solution. At low magnetic field, spontaneous conversion of p-H_2 spin order to enhanced longitudinal magnetization of the nuclear spins of the other ligands occurs. Subsequent complex dissociation results in hyperpolarized substrate molecules in solution. The lifetime of this complex plays a crucial role in attained SABRE NMR signal enhancements. Depending on the ligands, vastly different dissociation rates have been previously measured using EXSY or selective inversion experiments. However, both these approaches are generally time-consuming due to the long recycle delays (up to 2 min) necessary to reach thermal equilibrium for the nuclear spins of interest. In the cases of dilute solutions, signal averaging aggravates the problem, further extending the experimental time. Here, a new approach is proposed based on coherent hyperpolarization transfer to substrate protons in asymmetric complexes at high magnetic field. We have previously shown that such asymmetric complexes are important for application of SABRE to dilute substrates. Our results demonstrate that a series of high sensitivity EXSY spectra can be collected in a short experimental time thanks to the NMR signal enhancement and much shorter recycle delay.

1. Introduction

A widespread interest in hyperpolarization as a tool to overcome the sensitivity limitations of NMR spectroscopy has emerged over the last decade. Most popular hyperpolarization techniques in solution include dissolution dynamic nuclear polarization (dissolution DNP) [1–3], *para*-hydrogen induced polarization (PHIP) [4–8] and, recently introduced, Signal Amplification By Reversible Exchange (SABRE) [9–21].

Particularly, SABRE has attracted a great deal of attention due to the fast hyperpolarization (compared to dissolution DNP) and because it does not require chemical conversion of the substrates under investigation (such as in PHIP). SABRE provides enhanced nuclear spin polarization for small molecules in solution, based on their reversible interaction with *para*-hydrogen (p-H_2) at an iridium metal center. When such transient metal complex is formed at low magnetic field, transfer of spin order from the p-H_2-derived hydrides to the nuclear spins of the substrate molecule occurs via scalar couplings, resulting in strongly enhanced nuclear magnetization. Dissociation of the complex produces hyperpolarized substrate molecules in solution. The attainable NMR signal enhancement results from the interplay of scalar coupling interactions, longitudinal relaxation and lifetime of the transient metal complex [22,23]. Previous studies on SABRE complexes have revealed large variations in substrate dissociation rates [24,25] depending on the N-heterocyclic carbene (NHC) ligands. Also the structure of the substrates in the equatorial plane strongly influences the complex dissociation rate. For the first (symmetric) NHC-complex used, [Ir(IMes)(pyridine)$_3$(H)$_2$]Cl (IMes = (1,3-bis (2,4,6- trimethylphenyl)imidazole-2-ylidene)) relatively high pyridine dissociation rates ($\sim$12 s^{-1} at 300 K) were determined [10], reflected by polarization levels up to P(^{1}H) = 8% for pyridine *para*-protons [10], and P(^{15}N) = 24% for ^{15}N-labeled pyridine [19,20]. In contrast, the dissociation rate drops to $\sim$0.2 s^{-1} for asymmetric Ir (IMes) complexes containing a unit of 1-methyl-1,2,3-triazole (*mtz*) in the equatorial plane; as previously reported, this slower exchange strongly affects the maximal observed NMR signal enhancement [15].

The determination of the substrate exchange rate requires acquiring a series of 2D EXSY experiments for different durations of the exchange period Δ. Alternatively, the same information

* Corresponding author.
E-mail addresses: n.hermkens@science.ru.nl (N.K.J. Hermkens), M.Feiters@science.ru.nl (M.C. Feiters), f.rutjes@science.ru.nl (F.P.J.T. Rutjes), S.Wijmenga@nmr.ru.nl (S.S. Wijmenga), m.tessari@science.ru.nl (M. Tessari).

http://dx.doi.org/10.1016/j.jmr.2017.01.011
1090-7807/

can be obtained by measuring a series of 1D spectra at variable durations of Δ after selective magnetization inversion of the protons of unbound substrate. In both approaches the integrals of the free and bound substrate signals are fitted to the equations describing the exchange of longitudinal magnetization as a function of Δ (*see further*, Eq. (4)). In general, acquisition of such an exchange series is time consuming because of the long recovery delay necessary to attain thermal equilibrium at the beginning of each transient. Experiment times of 24 h or longer are not uncommon for substrates at sub-millimolar concentrations; such long-term stability requirement can represent a problem for some asymmetric Ir(IMes) complexes in solution.

Here, we present a more efficient approach for the determination of the substrate dissociation rate, based on the hyperpolarization of the hydrides in the iridium complex at high magnetic field. *Para*-hydrogen induced hyperpolarization has been previously exploited to investigate methal hydride exchange [26,27]. Here, enhanced substrate proton magnetization is obtained after a COSY-type coherence transfer from the hyperpolarized hydrides. We have previously shown that such COSY transfer can be applied to asymmetric iridium complexes, and allows rapid acquisition of NMR spectra for substrate molecules at sub-μM concentrations [28]. In a similar fashion, a magnetization transfer from the *p*-H_2 enhanced hydrides to ^{15}N-labelled pyridine was previously employed to investigate Crabtree complex dissociation rates [29]. We have extended this approach to the general case of unlabeled SABRE-substrates and show that incorporating such hyperpolarization scheme into 1D EXSY experiments allows fast recording of a complete exchange series. This NMR method was tested using pyridine as a model substrate at sub-mM concentration for two different iridium metal complexes.

2. Theory

2.1. Spin system

Hydrogenation of complex precursor [Ir(NHC-X)(COD)Cl] in the presence of an excess of substrate (sub) produces the octahedral SABRE complex [Ir(NHC-X)$(H)_2$$(sub)_3$]Cl, with two chemically equivalent hydrides occupying the symmetric equatorial plane (NHC-X denotes the IMES or SIMES = (1,3-bis(2,4,6-trimethylphenyl)-4,5-dihydroimidazole-2-ylidene) carbene ligands). The loss of magnetic equivalence within *p*-H_2 upon association to this metal complex allows for the conversion of the singlet order into enhanced longitudinal magnetization on the substrate protons. Note that this process occurs efficiently only if matching conditions are realized, as previously reported both at low and high magnetic field [30–33].

Alternatively, hyperpolarization via cross-relaxation has been demonstrated as a mechanism for SABRE at high magnetic field [34]. We have recently shown that at high magnetic field a COSY-type polarization transfer to substrate protons is also possible, albeit within asymmetric SABRE complexes [28]. Such complexes can be formed upon metal binding of a second substrate in the equatorial plane, resulting in the chemical inequivalence of the hydrides. In Fig. 1A the structure of the asymmetric [Ir(IMes)$(H)_2$(py)$(mtz)_2$]Cl and [Ir(SIMes)$(H)_2$(py)$(mtz)_2$]Cl complexes are sketched, obtained in the presence of pyridine (py) and a large excess of *mtz* as a second substrate.

2.2. NMR

P-H_2 spin order can be converted into enhanced in-phase hydride signals using a SEPP [35] (*s*elective *e*xcitation of *p*olarization using *P*ASADENA [36]) pulse scheme, where the upfield hydride H_A (spin I^A) is selectively excited with a shaped 90-degree pulse followed by a period δ_1 (Fig. 1B) to refocus the anti-phase coherence with respect to hydride H_X (spin I^X). Therefore, the duration of the refocusing period δ_1 should be taken as an odd multiple of $0.5/J_{AX}$. During the same period anti-phase coherence with respect to the substrate protons is created. As previously reported, for pyridine-like compounds this process involves mainly the *ortho* protons M via a long-range $^4J_{AM}$ coupling of approximately 1.2 Hz [37]. A pair of selective 90-degree pulses realizes a COSY-type transfer to the aromatic protons M (spin I^M). In the following period of duration δ_2, H_M antiphase coherence with respect to hydride H_A is refocused to produce in-phase magnetization. Note that the refocusing 180 degree pulse is selectively applied on the *ortho* protons H_M to prevent further dephasing due to scalar couplings to other aromatic protons (i.e. *meta* and *para* aromatic protons). In-phase coherence is converted to enhanced longitudinal magnetization of bound *ortho* protons; during the following period of variable duration Δ, substrate loss results in enhanced longitudinal magnetization of the *ortho* protons of substrate molecules free in solution. After this period, acquisition of the signals of *ortho* protons, both in free and bound form takes place. After bubbling *p*-H_2 through the solution at high magnetic field, the coherence flow can be described by means of product operator formalism as:

$$\begin{aligned} 2\hat{I}_z^A\hat{I}_z^X &\xrightarrow{\left(\frac{\pi}{2}\right)_x^{I^A}} -2\hat{I}_y^A\hat{I}_z^X \xrightarrow{\delta_1} 2\hat{I}_y^A\hat{I}_z^M \sin(\pi J_{AX}\delta_1)\sin(2\pi J_{AM}\delta_1) \\ &\times \xrightarrow{\left(\frac{\pi}{2}\right)_x^{I^A},\left(\frac{\pi}{2}\right)_x^{I^M}} -2\hat{I}_z^A\hat{I}_y^M \sin(2\pi J_{AM}\delta_1) \xrightarrow{\delta_2} \hat{I}_x^M \sin(2\pi J_{AM}\delta_1) \\ &\times \sin(\pi J_{AM}\delta_2) \xrightarrow{\left(\frac{\pi}{2}\right)_y^{I^M}} -\hat{I}_z^M \sin(2\pi J_{AM}\delta_1)\sin(\pi J_{AM}\delta_2) \end{aligned} \quad (1)$$

Although in principle several processes can affect the evolution of the proton magnetization during the exchange period Δ (see Results and Discussion), only two NMR signals are observed in the High-Field hyperpolarization-EXSY experiment, corresponding to the *ortho* protons of pyridine in the bound- and in the free form. Therefore, the evolution of the magnetization was modeled assuming a simple two-sites exchange process, described by:

$$\frac{d}{dt}\begin{bmatrix}\left\langle\hat{I}_z^{M,B}\right\rangle\\ \left\langle\hat{I}_z^{M,F}\right\rangle\end{bmatrix} = -\begin{bmatrix}\rho_B + k_{diss} & -k_{ass}^*\\ -k_{diss} & \rho_F + k_{ass}^*\end{bmatrix}\begin{bmatrix}\left\langle\hat{I}_z^{M,B}\right\rangle - I_{eq}^{M,B}\\ \left\langle\hat{I}_z^{M,F}\right\rangle - I_{eq}^{M,F}\end{bmatrix} \quad (2)$$

with

$$\left\langle\hat{I}_z^{M,B}\right\rangle \sim 100 \times \hat{I}_{eq}^{M,B}$$
$$\left\langle\hat{I}_z^{M,F}\right\rangle = 0$$

where ρ_B and ρ_F indicate the longitudinal relaxation rates of the *ortho* protons (M) in the bound and free form, respectively. The notation "B" and "F" refers to the bound and free states of the substrate molecules, respectively. The symbols k_{diss} and k_{ass}^* denote the rate constant for dissociation and the pseudo-rate constant for association of the substrate to the iridium complex, respectively. Please, consider that while the k_{diss} rate constant refers to a well defined first order dissociation process, the pseudo-rate constant for the reverse pathway (i.e. association) is not as straightforward to interpret, as it refers to a complex, multistep process.

The magnetization of the bound form at the beginning of the exchange period Δ is ca. 100 times larger than thermal magnetization. Eq. (2) describes the redistribution (and the decay) of this enhanced magnetization between bound and free form. Because of the phase cycling employed in this experiment, only signals originating from hyperpolarized hydrides are selected. Therefore, association of not-hyperpolarized pyridine to the iridium complex,

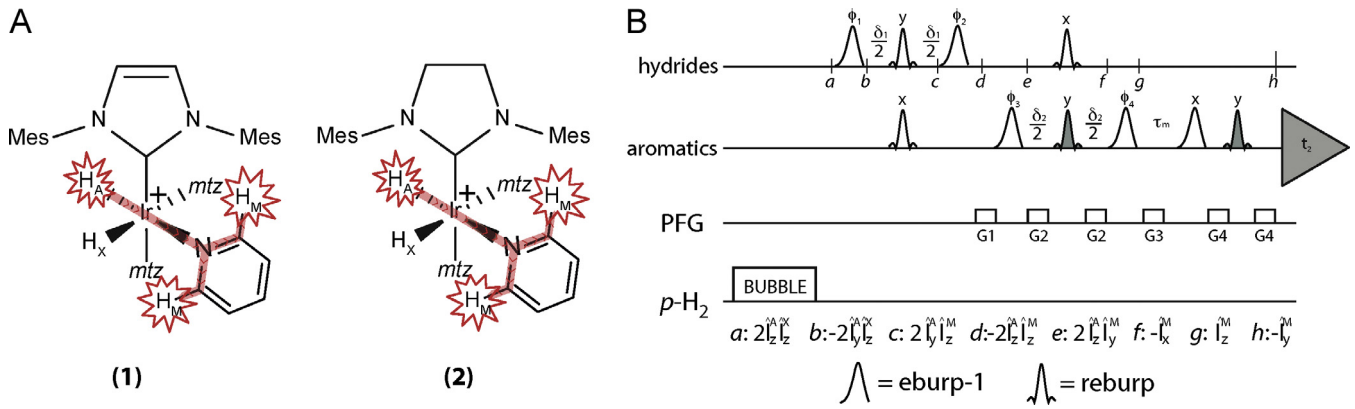

Fig. 1. (A) Schematic structure of the asymmetric [Ir(IMes)(H)$_2$(py)(mtz)$_2$]Cl and [Ir(SIMes)(H)$_2$(py)(mtz)$_2$]Cl SABRE metal complexes ((**1**) and (**2**) respectively). The conversion of longitudinal spin order from hydride A to magnetization of *ortho*-protons of pyridine, here taken as a model substrate, is indicated by the red lines. **(B)** High-Field hyperpolarization-EXSY pulse scheme for the determination of the substrate dissociation rate. The experiment makes use of a high-field hyperpolarizationt transfer from p-H$_2$ derived hydrides to the *ortho*-protons of pyridine. δ_1 = 183 ms; δ_2 = 100 ms. The coherence flow along the pulse scheme is illustrated in the main text. Relevant product operators at specific time points are indicated; note that the indices A and X refer to hydrides, while M denotes substrate protons. Phase cycling: ϕ_1 = x, −x; ϕ_2 = 2(x), 2(−x); ϕ_3 = 4(x), 4(−x); ϕ_4 = 8(y),8(−y); ϕ_{rec} = x, −x, −x, x, 2(−x, x, x, −x), x, −x, −x, x. Shaped pulses are eburp-1 for excitation, and reburp for refocusing/inversion. Greyed out reburp pulses are selectively applied to *ortho*-protons (bandwidth 450 Hz). Squared blocks indicate pulse-field gradients. P-H$_2$ was typically bubbled for 5 s, for a total interscan delay of 6 s.

as well as not-hyperpolarized substrate loss are not observed in the present experiment. Solution of (2) provides the time evolution of the longitudinal magnetization of the *ortho* protons during the period Δ:

$$I_z^{M,B}(\Delta) = K \times \left(e^{-\lambda_1 \Delta} - \frac{(\rho_B - \lambda_1)(\rho_F - \lambda_2)}{(\rho_F - \lambda_1)(\rho_B - \lambda_2)} e^{-\lambda_2 \Delta} \right) I_z^{M,B}(0)$$

$$I_z^{M,F}(\Delta) = -K \times \frac{(\rho_F - \lambda_2)}{(\rho_B - \lambda_2)} (e^{-\lambda_1 \Delta} - e^{-\lambda_2 \Delta}) I_z^{M,B}(0) \quad (3)$$

$$\lambda_1 = \rho_B + k_{diss} + \frac{\varepsilon}{2}$$

$$\lambda_2 = \rho_F + k_{ass}^* - \frac{\varepsilon}{2}$$

$$\varepsilon = \sqrt{(\rho_B - \rho_F + k_{diss} - k_{ass}^*)^2 + 4 k_{diss} k_{ass}^*} - (\rho_B - \rho_F + k_{diss} - k_{ass}^*)$$

In order to determine the exchange parameters, a series of hyperpolarized spectra at different duration of Δ must be acquired. Fitting the signal integrals of the protons M as a function of Δ using Eq. (3) provides exchange, as well as relaxation parameters. The solution of Eq. (2) in the case of a selective inversion experiment has the same functional form as (3):

$$\begin{aligned} I_z^{M,B}(\Delta) &= -K \times \tfrac{(\rho_F - \lambda_2)}{(\rho_B - \lambda_2)} (e^{-\lambda_1 \Delta} - e^{-\lambda_2 \Delta}) I_z^{M,F}(0) + I_{eq}^{M,B} \\ I_z^{M,F}(\Delta) &= K \times \left(-\tfrac{(\rho_B - \lambda_1)(\rho_F - \lambda_2)}{(\rho_F - \lambda_1)(\rho_B - \lambda_2)} e^{-\lambda_1 \Delta} + e^{-\lambda_2 \Delta} \right) I_z^{M,F}(0) + I_{eq}^{M,F} \end{aligned} \quad (4)$$

Note that the contribution of thermal magnetization is missing in Eq. (3). This is due to the phase cycling employed in the high field hyperpolarization-EXSY pulse scheme (see Fig. 1B and caption).

3. Results and discussion

As discussed in the previous section, the high-field hyperpolarization-EXSY experiment requires bubbling p-H$_2$ into the sample at the beginning of each transient for a period sufficiently long to maximize the enhancement of the hydrides (typically between 500 and 1000 at room temperature for asymmetric complexes containing *mtz* as co-substrate). After bubbling, hydrides spin order is converted into enhanced longitudinal magnetization of the *ortho*-protons of the substrate using a refocused COSY-type transfer. The substrate magnetization enhancement is strongly dependent on the long-range scalar coupling interactions and on proton relaxation in the complex. Furthermore, complex dissociation during the refocused COSY transfer determines a reduction in the attained enhanced longitudinal magnetization. For the system investigated in the present work, the hyperpolarization transfer occurred via a long-range coupling of ca. 1.2 Hz, producing magnetization enhancements between 50 and 100 for the aromatic protons in the bound form. However, transfer schemes similar to the one proposed here have been previously implemented employing scalar coupling as small as ca. 0.4 Hz [37].

During the following time period Δ exchange of longitudinal magnetization occurs, reflecting the possible dissociation pathways of complexes (1) and (2). As far as H$_2$ loss is concerned, a number of detailed studies [10,25] on SABRE complexes has indicated this process does not occur via direct dissociation. Rather, H$_2$ loss is a multistep process that requires substrate dissociation and formation of a short-lived methanol adduct to proceed. Therefore, for the systems here investigated, the pathway leading to H$_2$ loss is not observable with the proposed scheme and does not need to be further considered. An additional dissociation pathway is represented by *mtz* loss from (1) and (2) which would lead to the formation of a methanol adduct containing hyperpolarized substrate. However, previous studies [25] have demonstrated that the population of such adduct is low (ca. 1%) when the ligand excess is large, as in the present case (1:15). The experimental observation that no NMR signal is observed other than the ones corresponding to bound and free substrate protons, confirms that the concentrations of other complexes containing hyperpolarized substrate is negligible for the systems under investigation.

High-field hyperpolarization-EXSY experiments were performed on complexes (**1**) and (**2**) at different durations of the exchange period Δ for a total experiment time of ca. 10 min per series. The signals of the *ortho*-protons for both free and bound pyridine obtained with the high-field hyperpolarization-EXSY pulse scheme in the case of complex (**2**) are shown in Fig. 2A for increasing duration of the delay Δ. Although these NMR experiments were conducted on a relatively dilute solution of pyridine (250 μM), a high signal-to-noise ratio was obtained, thanks to the sensitivity offered by hyperpolarization. In order to obtain quantitatively accurate data it is crucial that a steady state is

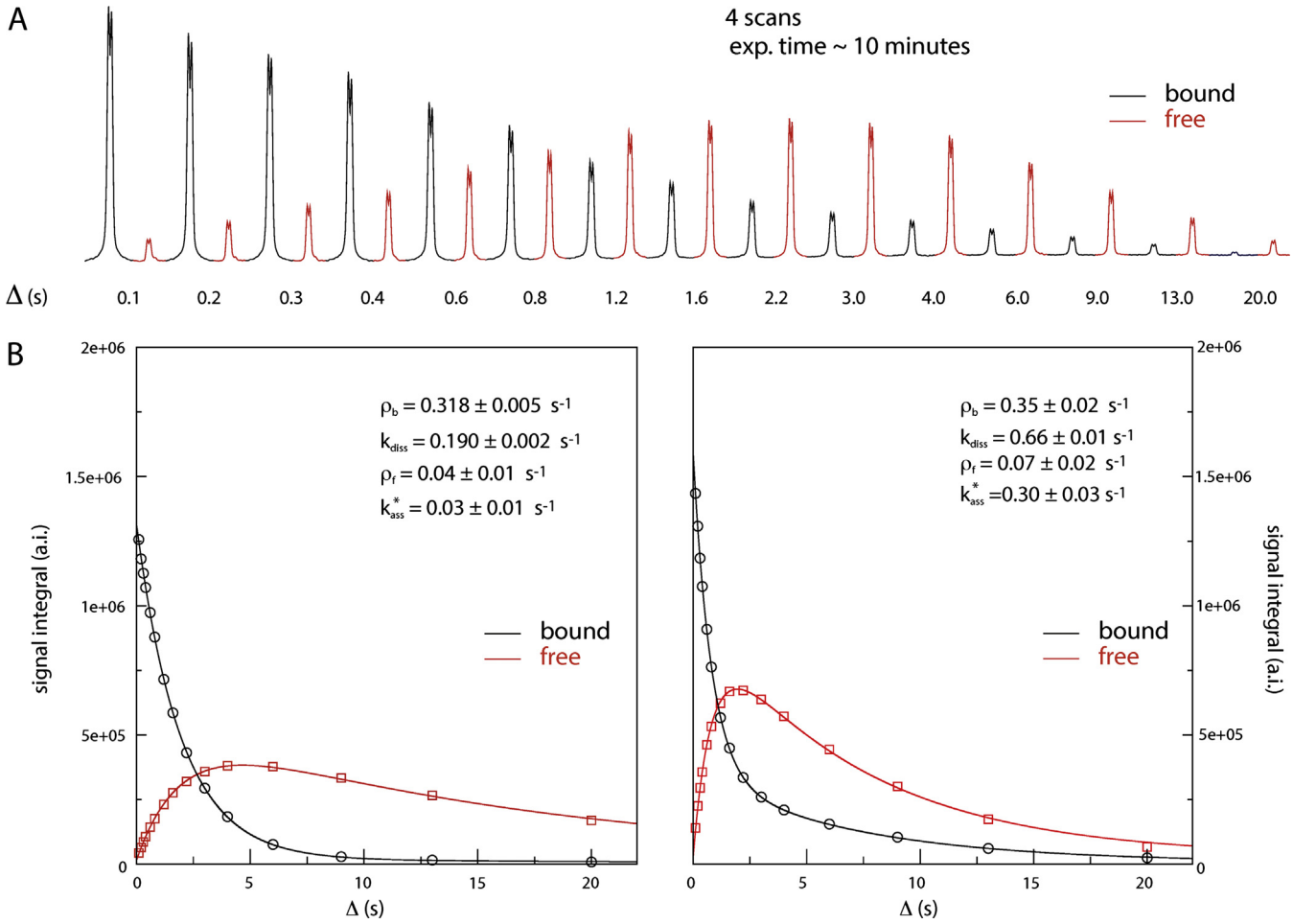

Fig. 2. **(A)** Signals of *ortho* protons of free- (red line) and bound- (black line) pyridine obtained with the high-field hyperpolarization-EXSY experiment using the metal complex (**2**). **(B)** Simultaneous fit of the signal integrals of *ortho* protons for free- (red square) and bound- (black circles) pyridine from high field hyperpolarization EXSY experiments using the metal complexes Ir(IMes) (**1**, left hand side) or Ir(SIMes) (**2**, right hand side). Each series was recorded in ca. 10 min using a solution of 1.2 mM metal complex, 18 mM mtz, 250 μM py dissolved in methanol-d_4 in the presence of 5 bar 51% enriched *p*-H_2. The duration of the exchange period (Δ) is indicated for both series. Dissociation rates of 0.19 s^{-1} and 0.66 s^{-1} were obtained for pyridine in the complexes (**1**) and (**2**), respectively, from the fits of five consecutive measurementes. All NMR experiments were performed on a Varian UnityInova spectrometer operating at 500 MHz, ^{1}H resonance frequency.

reached at the beginning of each transient, irrespective of the duration of the exchange period Δ. We found that this condition was met only when the sample was bubbled with *p*-H_2 (51%) for at least 5 s at the beginning of each transient. Signal integrals from the high field hyperpolarization series for complexes (**1**) and (**2**) are displayed in Fig. 2B as a function of the delay Δ, together with the curves obtained by fitting the experimental data with Eq. (3). Kinetic and relaxation parameters obtained as averages from five consecutive measurements are displayed in Fig. 2; these values are in good agreement with previous estimates [15] from selective inversion experiments. The faster dissociation in complex (**2**) allows for more efficient *p*-H_2 binding to the complex and hyperpolarization transfer to free pyridine. This is reflected in the observed signal increase for free pyridine, compared to complex (**1**).

Note that the fitting parameters relative to the free form (e.g. longitudinal relaxation rate ρ_F and association pseudo constant k^*_{ass}) are somewhat less well defined, particularly in the case of complex (**1**), for which a slower exchange kinetics was determined [15]. This results from the fact that only the dissociation pathway is well monitored by this experiment, as only substrate protons in the bound form can be hyperpolarized via COSY transfer from the hydrides. Conversely, the contribution of the reverse pathway (e.g. association) is less important, particularly for short durations of the exchange period Δ at which the concentration of unbound hyperpolarized substrate is very low. This is not the case for the standard selective-inversion experiment, in which both pathways (dissociation and association) contribute to the observed signal in a comparable fashion.

4. Conclusions

We have presented an efficient approach for the experimental determination of the substrate dissociation rate in asymmetric SABRE complexes. The proposed experiment does not require ^{15}N labeling of SABRE substrates and can be efficiently applied to dilute solutions. This technique was tested using pyridine as model substrate, in combination with mtz as co-substrate and iridium-IMes or iridium-SIMES as metal complexes. For the model system (py-mtz) here considered, values of ~0.19 s^{-1} and 0.66 s^{-1} were obtained for pyridine dissociation rate in Ir(IMes) and Ir(SIMes), respectively, which is in agreement with previously reported estimates [15]. The proposed approach has been successfully applied for dissociation rates ranging between ca. 0.1 s^{-1} and 3 s^{-1}; for much slower dissociation processes, longitudinal relaxation of the substrate proton magnetization strongly limits the transfer of magnetization to the free substrate. Conversely, for much faster complex dissociation rates the efficiency of the COSY-transfer

drops, reducing the experiment sensitivity and the gain offered by hyperpolarization.

We have previously demonstrated that asymmetric complexes are important to detect and quantify dilute N-heteroaromatic compounds in solution via high-field *p*-H_2 hyperpolarization chemoselective experiments [38,39]. The combination of NMR signal enhancement and short recycle delay has allowed acquisition of a complete series of hyperpolarization-EXSY experiments within 10 min at sub-mM substrate concentration, a ca. 100-fold reduction in experimental time compared to standard approaches. The applicability of the experiment presented here is not limited to N-heteroaromatic substrates, but it is expected to work on other classes of compounds capable of weakly associate to the iridium center, such as Schiff Bases [40], diazirines [41], and sulfur-based heterocycles [42]. Furthermore, in the context of hyperpolarization the experiment could be adapted to investigate SABRE enhancement of other nuclear spins [43–45].

5. Experimental

5.1. Chemicals

[Ir(IMes)(COD)Cl] (IMes-**p**), [Ir(SIMes)(COD)Cl] (SIMes-**p**) and 1-methyl-1,2,3-triazole (mtz) were synthesized according to published methods [46,47]. Pyridine (py) and methanol-d_4 were purchased from Sigma-Aldrich and Cambridge Isotope Laboratories, respectively, and used as supplied. *Para*-hydrogen (*p*-H_2) was prepared by cooling normal hydrogen gas (purity 5.0) down to 77 K in the presence of activated charcoal. The resulting 51% enriched *p*-H_2 was transferred to an aluminum cylinder with an adjustable output-pressure valve.

5.2. Sample preparation

Active SABRE complexes [Ir(IMes)$(H)_2$$(mtz)_2$(py)]Cl (**1**) and [Ir(SIMes)$(H)_2$$(mtz)_2$(py)]Cl (**2**), (see Fig. 1A) are formed upon hydrogenation of IMes-**p**, and SIMES-**p**, respectively, dissolved in methanol-d_4 to a concentration of 1.2 mM, in the presence of 18 mM mtz and 250 μM py.

5.3. Bubbling setup

Solutions were transferred to a 5 mm Wilmad quick pressure valve NMR tube sealed with an in-house built headpiece to which three PEEK tube lines are connected. At the beginning of each transient the headspace above the sample was depressurized to 4 bar through a vent line (250 ms), allowing efficient bubbling of p-H_2 (5 s) through the solution to a final pressure up to 5 bar. A backpressure was applied to quickly stop the bubbling (500 ms), followed by a recovery delay of 200 ms prior to the NMR pulse sequence. The vent-, bubble-, and backpressure delays are spectrometer-controlled through solenoid valves connected to the console.

5.4. NMR experiments

NMR experiments were carried out on a Varian Unity INOVA spectrometer equipped with a cryo-cooled insert, operating at a proton resonance frequency of 500 MHz. After full activation of the complex precursor (ca. 2 h for (**1**) and 15 min for (**2**)), the high-field hyperpolarization EXSY series was acquired with four transients per experiment, randomizing the order of acquisition with respect to the Δ delay. Signal integrals were fitted with Eq. (3) using in-house written routines implemented in Octave [48].

References

[1] J.H. Ardenkjær-Larsen, B. Fridlund, A. Gram, G. Hansson, L. Hansson, M.H. Lerche, R. Servin, M. Thaning, K. Golman, Increase in signal-to-noise ratio of >10,000 times in liquid-state NMR, Proc. Natl. Acad. Sci. USA 100 (2003) 10158.

[2] J. Wolber, F. Ellner, B. Fridlund, A. Gram, H. Jóhannesson, G. Hansson, L.H. Hansson, M.H. Lerche, S. Månsson, R. Servin, M. Thaning, K. Golman, J.H. Ardenkjær-Larsen, Generating highly polarized nuclear spins in solution using dynamic nuclear polarization, Nucl. Instrum. Methods Phys. Res., Sect. A 526 (2004) 173.

[3] L. Frydman, D. Blazina, Ultrafast two-dimensional nuclear magnetic resonance spectroscopy of hyperpolarized solutions, Nat. Phys. 3 (2007) 415.

[4] C.R. Bowers, D.P. Weitekamp, Transformation of symmetrization order to nuclear-spin magnetization by chemical-reaction and nuclear-magnetic-resonance, Phys. Rev. Lett. 57 (1986) 2645.

[5] M.G. Pravica, D.P. Weitekamp, TNet NMR alignment by adiabatic transport of parahydrogen addiction products to high magnetic field, Chem. Phys. Lett. 145 (1988) 255.

[6] K.V. Kovtunov, I.E. Beck, V.I. Bukhtiyarov, I.V. Koptyug, Observation of parahydrogen-induced polarization in heterogeneous hydrogenation on supported metal catalysts, Angew. Chem. Int. Ed. 47 (2008) 1492.

[7] M. Roth, P. Kindervater, H.-P. Raich, J. Bargon, H.W. Spiess, K. Münnemann, A nanoparticle catalyst for heterogeneous phase para-hydrogen-induced polarization in water, Angew. Chem. Int. Ed. 49 (2010) 8358.

[8] T.C. Eisenschmid, R.U. Kirss, P.P. Deutsch, S.I. Hommeltoft, R. Eisenberg, J. Bargon, R.G. Lawler, A.L. Balch, Para hydrogen induced polarization in hydrogenation reactions, J. Am. Chem. Soc. 109 (1987) 8089.

[9] R.W. Adams, J.A. Aguilar, K.D. Atkinson, M.J. Cowley, P.I.P. Elliott, S.B. Duckett, G.G.R. Green, I.G. Khazal, J. Lopez-Serrano, D.C. Williamson, Reversible interactions with para-hydrogen enhance NMR sensitivity by polarization transfer, Science 323 (2009) 1708.

[10] M.J. Cowley, R.W. Adams, K.D. Atkinson, M.C.R. Cockett, S.B. Duckett, G.G.R. Green, J.A.B. Lohman, R. Kerssebaum, D. Kilgour, R.E. Mewis, Iridium N-heterocyclic carbene complexes as efficient catalysts for magnetization transfer from para-hydrogen, J. Am. Chem. Soc. 133 (2011) 6134.

[11] S. Glöggler, R. Müller, J. Colell, M. Emondts, M. Dabrowski, B. Blümich, S. Appelt, Para-hydrogen induced polarization of amino acids, peptides and deuterium-hydrogen gas, Phys. Chem. Chem. Phys. 13 (2011) 13759.

[12] E.B. Dücker, L.T. Kuhn, K. Münnemann, C. Griesinger, Similarity of SABRE field dependence in chemically different substrates, J. Magn. Reson. 214 (2012) 159.

[13] L.S. Lloyd, R.W. Adams, M. Bernstein, S. Coombes, S.B. Duckett, G.G.R. Green, R. J. Lewis, R.E. Mewis, C.J. Sleigh, Utilization of SABRE-derived hyperpolarization to detect low-concentration analytes via 1D and 2D NMR methods, J. Am. Chem. Soc. 134 (2012) 12904.

[14] J.B. Hövener, N. Schwaderlapp, T. Lickert, S.B. Duckett, R.E. Mewis, L.A.R. Highton, S.M. Kenny, G.G.R. Green, D. Leibfritz, J.G. Korvink, J. Hennig, D. von Elverfeldt, A hyperpolarized equilibrium for magnetic resonance, Nat. Commun. 4 (2013) 2946.

[15] N. Eshuis, N. Hermkens, B.J.A. van Weerdenburg, M.C. Feiters, F.P.J.T. Rutjes, S. S. Wijmenga, M. Tessari, Toward nanomolar detection by NMR through SABRE hyperpolarization, J. Am. Chem. Soc. 136 (2014) 2695.

[16] F. Shi, A.M. Coffey, K.W. Waddell, E.Y. Chekmenev, B.M. Goodson, Heterogeneous solution NMR signal amplification by reversible exchange, Angew. Chem. Int. Ed. 53 (2014) 7495.

[17] H. Zeng, J. Xu, M.T. McMahon, J.A.B. Lohman, P.C.M. van Zijl, Achieving 1% NMR polarization in water in less than 1 min using SABRE, J. Magn. Reson. 246 (2014) 119.

[18] N. Eshuis, B.J.A. van Weerdenburg, M.C. Feiters, F.P.J.T. Rutjes, S.S. Wijmenga, M. Tessari, Quantitative trace analysis of complex mixtures using SABRE hyperpolarization, Angew. Chem. Int. Ed. 54 (2015) 1481.

[19] T. Theis, M.L. Truong, A.M. Coffey, R.V. Shchepin, K.W. Waddell, F. Shi, B.M. Goodson, W.S. Warren, E.Y. Chekmenev, Microtesla SABRE enables 10% nitrogen-15 nuclear spin polarization, J. Am. Chem. Soc. 137 (2015) 1404.

[20] D.A. Barskiy, R.V. Shchepin, A.M. Coffey, T. Theis, W.S. Warren, B.M. Goodson, E. Y. Chekmenev, Over 20% ^{15}N hyperpolarization in under one minute for metronidazole, an antibiotic and hypoxia probe, J. Am. Chem. Soc. 138 (2016) 8080.

[21] V. Daniele, F.X. Legrand, P. Berthault, J.N. Dumez, G. Huber, Single-scan multidimensional NMR analysis of mixtures at sub-millimolar concentrations using SABRE hyperpolarization, ChemPhysChem 16 (2015) 3413.

[22] D.A. Barskiy, A.N. Pravdivtsev, K.L. Ivanov, K.V. Kovtunov, I.V. Koptyug, A simple analytical model for signal amplification by reversible exchange (SABRE) process, Phys. Chem. Chem. Phys. 18 (2016) 89.

[23] S. Knecht, A.N. Pravdivtsev, J.B. Hövener, A.V. Yurkovskay, K.L. Ivanov, Quantitative description of the SABRE process: rigorous consideration of spin dynamics and chemical exchange, RSC Adv. 6 (2016) 24470.

[24] B.J.A. van Weerdenburg, S. Glöggler, N. Eshuis, A.H.J. Engwerda, J.M.M. Smits, R. de Gelder, S. Appelt, S.S. Wymenga, M. Tessari, M.C. Feiters, B. Blumich, F.P.J.T. Rutjes, Ligand effects of NHC-iridium catalysts for signal amplification by reversible exchange (SABRE), Chem. Commun. 49 (2013) 7388.

[25] L.S. Lloyd, A. Asghar, M.J. Burns, A. Charlton, S. Coombes, M.J. Cowley, G.J. Dear, S.B. Duckett, G.R. Genov, G.G.R. Green, L.A.R. Highton, A.J.J. Hooper, M. Khan, I. G. Khazal, R.J. Lewis, R.E. Mewis, A.D. Roberts, A.J. Ruddlesden, Hyperpolarisation through reversible interactions with parahydrogen, Catal. Sci. Technol. 4 (2014) 3544.

[26] D. Blazina, S.B. Duckett, P.J. Dyson, B.F.G. Johnson, J.A.B. Lohman, C.J. Sleigh, NMR studies of Ru-3(CO)(10)(PMe2Ph)(2) and Ru-3(CO)(10)(PPh3)(2) and their H-2 addition products: detection of new isomers with complex dynamic behavior, J. Am. Chem. Soc. 123 (2001) 9760.
[27] S.A. Colebrooke, S.B. Duckett, J.A.B. Lohman, R. Eisenberg, Hydrogenation studies involving halobis(phosphine)-rhodium(I) dimers: use of parahydrogen induced polarisation to detect species present at low concentration, Chem. Eur. J. 10 (2004) 2459.
[28] N. Eshuis, R.L.E.G. Aspers, B.J.A. van Weerdenburg, M.C. Feiters, F.P.J.T. Rutjes, S. S. Wijmenga, M. Tessari, 2D NMR trace analysis by continuous hyperpolarization at high magnetic field, Angew. Chem. Int. Ed. 54 (2015) 14527.
[29] K.D. Atkinson, M.J. Cowley, S.B. Duckett, P.I. Elliott, G.G. Green, J. Lopez-Serrano, I.G. Khazal, A.C. Whitwood, Para-hydrogen induced polarization without incorporation of para-hydrogen into the analyte, Inorg. Chem. 48 (2009) 663.
[30] A.N. Pravdivtsev, A.V. Yurkovskaya, H.M. Vieth, K.L. Ivanov, R. Kaptein, Level anti-crossings are a key factor for understanding para-hydrogen-induced hyperpolarization in SABRE experiments, ChemPhysChem 14 (2013) 3327.
[31] A.N. Pravdivtsev, A.V. Yurkovskaya, H.M. Vieth, K.L. Ivanov, Spin mixing at level anti-crossings in the rotating frame makes high-field SABRE feasible, Phys. Chem. Chem. Phys. 16 (2014) 24672.
[32] A.N. Pravdivtsev, A.V. Yurkovskaya, H.M. Vieth, K.L. Ivanov, RF-SABRE: a way to continuous spin hyperpolarization at high magnetic fields, J. Phys. Chem. B 119 (2015) 13619.
[33] T. Theis, M. Truong, A.M. Coffey, E.Y. Chekmenev, W.S. Warren, LIGHT-SABRE enables efficient in-magnet catalytic hyperpolarization, J. Magn. Reson. 248 (2014) 23.
[34] D.A. Barskiy, K.V. Kovtunov, I.V. Koptyug, P. He, K.A. Groome, Q.A. Best, F. Shi, B. M. Goodson, R.V. Shchepin, A.M. Coffey, K.W. Waddell, E.Y. Chekmenev, The feasibility of formation and kinetics of NMR signal amplification by reversible exchange (SABRE) at high magnetic field (9.4 T), J. Am. Chem. Soc. 136 (2014) 3322.
[35] H. Sengstschmid, R. Freeman, J. Barkemeyer, J. Bargon, A new excitation sequence to observe the PASADENA effect, J. Magn. Reson., Ser. A 120 (1996) 249.
[36] C.R. Bowers, D.P. Weitekamp, Parahydrogen and synthesis allow dramatically enhanced nuclear alignment, J. Am. Chem. Soc. 109 (1987) 5541.
[37] N. Eshuis, R.L.E.G. Aspers, B.J.A. van Weerdenburg, M.C. Feiters, F.P.J.T. Rutjes, S. S. Wijmenga, M. Tessari, Determination of long-range scalar $^{1}H–^{1}H$ coupling constants responsible for polarization transfer in SABRE, J. Magn. Reson. 265 (2016) 59.
[38] N.K.J. Hermkens, N. Eshuis, B.J.A. van Weerdenburg, M.C. Feiters, F.P.J.T. Rutjes, S.S. Wijmenga, M. Tessari, NMR-based chemosensing via p-H_2 hyperpolarization: application to natural extracts, Anal. Chem. 88 (2016) 3406.
[39] I. Reile, N. Eshuis, N.K.J. Hermkens, B.J.A. van Weerdenburg, M.C. Feiters, F.P.J.T. Rutjes, M. Tessari, NMR detection in biofluid extracts at sub-mu M concentrations via para-H-2 induced hyperpolarization, Analyst 141 (2016) 4001.
[40] A.W.J. Logan, T. Theis, J.F.P. Colell, W.S. Warren, S.J. Malcolmson, Hyperpolarization of nitrogen-15 schiff bases by reversible exchange catalysis with para-hydrogen, Chem. Eur. J. 22 (2016) 10777.
[41] T. Theis, G.X. Ortiz Jr., A.W.J. Logan, K.E. Claytor, Y. Feng, W.P. Huhn, V. Blum, S. J. Malcolmson, E.Y. Chekmenev, Q. Wang, W.S. Warren, Direct and cost-efficient hyperpolarization of long-lived nuclear spin states on universal $^{15}N2$-diazirine molecular tags, Sci. Adv. 2 (2016) e1501438.
[42] R.V. Shchepin, D.A. Barskiy, A.M. Coffey, B.M. Goodson, E.Y. Chekmenev, NMR signal amplification by reversible exchange of sulfur-heterocyclic compounds found in petroleum, Chem. Select 1 (2016) 2552.
[43] V.V. Zhivonitko, I.V. Skovpina, I.V. Koptyug, Strong ^{31}P nuclear spin hyperpolarization produced via reversible chemical interaction with parahydrogen, Chem. Commun. 51 (2015) 2506.
[44] A.M. Olaru, A. Burt, P.J. Rayner, S.J. Hart, A.C. Whitwood, G.G.R. Green, S.B. Duckett, Using signal amplification by reversible exchange (SABRE) to hyperpolarise 119Sn and 29Si NMR nuclei, Chem. Commun. 52 (2016) 14482.
[45] M.L. Truong, T. Theis, A.M. Coffey, R.V. Shchepin, K.W. Waddell, F. Shi, B.M. Goodson, W.S. Warren, E.Y. Chekmenev, ^{15}N hyperpolarization by reversible exchange using SABRE-SHEATH, J. Phys. Chem. C 119 (2015) 8786.
[46] M.A. Seefeld, M.B. Rouse, D.A. Heerding, S. Peace, D.S. Yamashita, K.C. McNulty, Inhibitors of AKT Activity, WO 2008/098104 A1, 14 August 2008.
[47] R.A. Kelly III, H. Clavier, S. Giudice, N.M. Scott, E.D. Stevens, J. Bordner, I. Samardjiev, C.D. Hoff, L. Cavallo, S.P. Nolan, Determination of N-heterocyclic carbene (NHC) steric and electronic parameters using the [(NHC)Ir(CO)2Cl] system, Organometallics 27 (2008) 202.
[48] John W. Eaton, David Bateman, Søren Hauberg, Gnu Octave Version 3.0.1 Manual: A High-Level Interactive Language for Numerical Computations 1st Edition, 2009.